

# NOVEL METHODS FOR EXPERIMENTAL CHARACTERIZATION OF 3D SUPERCONDUCTING LINAC BEAM DYNAMICS

A. Shishlo<sup>#</sup>, ORNL, Oak Ridge, TN 37831, USA

## Abstract

This paper describes an approach to measure initial Twiss parameters in transverse and longitudinal directions at the entrance of a linac with independent short accelerating cavities. For the transverse plane the usual technique of transverse profiles is used, and for the longitudinal direction a recently developed non-intercepting method is applied. The new method is based on a beam position monitor amplitudes analysis. The applicability of the methods are discussed and demonstrated on an example of the Spallation Neutron Source superconducting linac.

## INTRODUCTION

Beam loss in accelerators should be low enough to allow “hands on” maintenance. This goal is achieved by a good design of the machine and a precise tuning before the operation phase. According to its design, the superconducting linac (SCL) of the Spallation Neutron Source (SNS) accelerator should be a almost loss-free part of the machine due to large apertures and low residual gas pressure. During the commissioning, it was found that SCL had significant beam loss and could be activated above the “hands on” maintenance level when the beam power reaches a design value of 1.4 MW. Fortunately, this beam loss was reduced to an acceptable level by reducing the strength of the quadrupoles in the SCL without a clear understanding the loss mechanism. After that, the power of SNS accelerator was not limited by SCL beam loss. Recently, the SCL beam loss mechanism was identified as intra-beam stripping (IBSt) [1,2]. IBSt is a process of stripping one loosely-bound electron from one of two H<sup>+</sup> ions colliding inside the bunch. The neutral hydrogen atom created in this collision will not see any focusing fields, and it will be lost on the beam pipe. The reaction rate of IBSt is proportional to the square of the particle bunch density, so the reducing of the SCL quadrupole strengths made the beam bigger transversely and reduced the density and beam loss. The process of a quadrupole focusing fields tuning is and was a purely empirical beam loss reduction based on readings of Beam Loss Monitors (BLM). All previous attempt to use a model based approach to the SCL loss reduction failed, and this paper is an attempt to explain why we did not succeeded before.

## RATIONALE

IBSt beam loss is defined by the core of the bunch where the most particles are located. It allows us to describe this loss with a simple envelope model instead of

complicated and slow particle-in-cell tracking codes. After certain assumptions (the Gaussian particles distribution in the bunch), the only parameters needed for the loss calculation are Twiss parameters of the bunch for all three directions along the linac [1]. To calculate these Twiss parameters we need the following components:

- A validated envelope tracking accelerator model.
- The measured initial Twiss parameters for all three dimensions.

The present work describes how to get these components for the SNS superconducting linac tuning. The problem of loss reduction based on this model and the initial Twiss parameters is a subject of future studies.

## THE SNS SUPERCONDUCTING LINAC

The SNS superconducting linac consists of Medium and High Beta sections named in accordance with the two types of superconducting cavities designed for geometrical relativistic  $\beta=0.61$  and  $0.81$  beams. The first section has 11 cryomodules with 3 cavities in each module, and the High Beta section has 12 modules, 4 cavities per module. Each 805 MHz cavity has independent control of the field gradient and phase. According to the design, the cavity field gradients in each section should be all the same, but in reality they are not. Instead, the gradient of each cavity is set to be as high as possible for stable operation. The input energy of the SCL is 185.6 MeV; the output energy is about 930 MeV, and it is defined by existing cavity gradients; the design peak current is 38 mA and the design energy 1 GeV. The bunch frequency of 402.5 MHz is defined by a normal conducting part of the linac. The SCL has 32 stripline beam position monitors (BPMs) installed along the linac between cryomodules and in the cavity-free part of SCL. The BPMs measure the transverse positions of the beam, the arrival phases of the bunches, and the amplitudes of the Fourier harmonics of the bunch longitudinal distributions at the bunch frequency. The SCL is also equipped with 9 Laser Wire (LW) Stations to measure transverse profiles of the beam. Four LWs are installed at the beginning of each of the two sections (one LW after each of the first four superconducting cavities) and one LW at the end of SCL.

## XAL ONLINE MODEL

All simulations and analysis performed for this work used the XAL Online Model (OM) [3]. The OM is an envelope tracking accelerator code similar to TRACE3D [4]. The OM tracks the envelope parameters through the SCL lattice using transport matrices for each quadrupole, each RF gap in the accelerating cavities, and each drift space. The space charge kicks are accumulated in the total

<sup>#</sup> shishlo@ornl.gov

transport matrix describing the transformation of the envelope from the beginning to an arbitrary point in SCL. The parameters of the lattice, such as the quadrupole field gradients, are taken from the control system. The field gradients and phases of the superconducting cavities are found after an analysis of the phase scans. The cavity phase scan is a process of collecting the BPM phases and amplitudes for a cavity phase changing from  $-180^0$  to  $+180^0$ . All downstream cavities have the RF pulse blanked so they will not affect the beam, and the number of bunches in the pulse train is limited to about 200 to avoid beam loading of the cavities. Figure 1 shows the results of a phase scan of the first SCL cavity Cav01a. The phase difference between two BPMs are analysed as a time-of-flight measurement to get the amplitude of the cavity in the online model and the phase of its first accelerating gap. The phase set-point of each cavity was chosen to be  $18^0$  less than the position of the maximal acceleration (see Fig. 1). These settings are usual for the production tune of SCL.

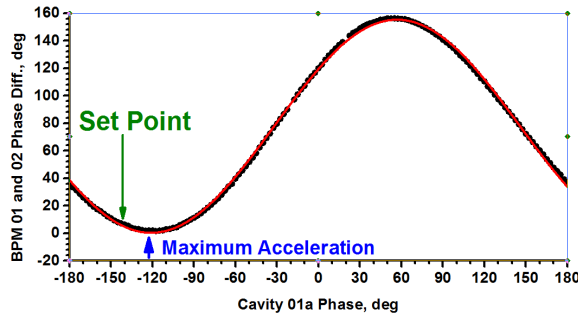


Figure 1: The BPM 01 and 02 phase difference during the phase scan of the first SCL cavity. Points are measurements, and the red line is an OM simulation.

After the online model lattice is initialized we can start the procedure of measuring the initial Twiss parameters for the transverse and longitudinal directions. In the presence of space charge forces these tasks are coupled, and they should be performed by iterations. We intend to do this in the future, but here we present analyses of the transverse and longitudinal data that were acquired about one year apart just to demonstrate the applicability of the methods. We will start with the algorithm and data analysis for horizontal and vertical directions.

## TRANSVERSE PROFILES ANALYSIS

To get the initial Twiss for the horizontal and vertical directions from multiple profile measurements we will use the techniques described in [5]. Let's consider one direction. The transformation coordinates of the particle between the beginning of the lattice and the profile measurement device are defined by the transport matrix from the envelope model

$$\begin{pmatrix} x_1 \\ x_1' \end{pmatrix} = \begin{bmatrix} m_{11}^{(1)} & m_{12}^{(1)} \\ m_{21}^{(1)} & m_{22}^{(1)} \end{bmatrix} \cdot \begin{pmatrix} x_0 \\ x_0' \end{pmatrix}, \quad (1)$$

where  $x_0, x_0'$  and  $x_1, x_1'$  are coordinates of the particle at points 0 and 1, and  $m^{(1)}$  is a transport matrix. By

calculating the square of both sides of the first equation of the (1) system and averaging over the whole ensemble of particles in the bunch, we have the expression for the squared RMS beam size  $\langle x_1^2 \rangle$

$$\langle x_1^2 \rangle = (m_{11}^{(1)})^2 \langle x_0^2 \rangle + 2m_{11}^{(1)}m_{12}^{(1)} \langle x_0 x_0' \rangle + (m_{12}^{(1)})^2 \langle x_0'^2 \rangle,$$

where  $\langle x_0^2 \rangle$ ,  $\langle x_0 x_0' \rangle$ , and  $\langle x_0'^2 \rangle$  are the correlations of the coordinates for the initial state. By using several profile monitors or modifying the optics of the lattice we can get as many different transport matrices  $m^{(i)}, i = 1, \dots, N$  and equations for the beam RMS sizes as we want. All this information can be represented by the following matrix equation

$$\begin{bmatrix} \langle x_1^2 \rangle \\ \dots \\ \langle x_N^2 \rangle \end{bmatrix} = \begin{bmatrix} m_{11}^{(1)2} & 2m_{11}^{(1)}m_{12}^{(1)} & m_{12}^{(1)2} \\ \dots & \dots & \dots \\ m_{11}^{(N)2} & 2m_{11}^{(N)}m_{12}^{(N)} & m_{12}^{(N)2} \end{bmatrix} \cdot \begin{bmatrix} \langle x_0^2 \rangle \\ \langle x_0 x_0' \rangle \\ \langle x_0'^2 \rangle \end{bmatrix}. \quad (2)$$

Assuming we have the measured RMS beam sizes  $s_1, s_2, \dots, s_N$  we can find the initial correlations  $\langle x_0^2 \rangle$ ,  $\langle x_0 x_0' \rangle$ , and  $\langle x_0'^2 \rangle$  by minimizing the sum

$$S = \sum_{i=1}^N \frac{(s_i^2 - \langle x_i^2 \rangle)^2}{\sigma_i^2}, \quad (3)$$

where  $\sigma_i$  denotes the rms error of the measured  $s_i^2$ . This error is obtained from the fit to the  $i$ -th profile which determines  $s_i$ .

The equation (3) is a typical linear Least Square Method problem, and the solution is

$$\begin{bmatrix} \langle x_0^2 \rangle \\ \langle x_0 x_0' \rangle \\ \langle x_0'^2 \rangle \end{bmatrix} = (M^T W M)^{-1} M^T W \begin{bmatrix} s_1^2 \\ \dots \\ s_N^2 \end{bmatrix}, \quad (4)$$

where  $M$  is  $N \times n$  matrix from equation (2) and  $W$  is a diagonal weight matrix

$$W_{ii} = 1/\sigma_i^2. \quad (5)$$

A symmetric 3 x 3 covariance matrix

$$C = (M^T W M)^{-1} \quad (6)$$

defines the errors for the initial correlation values found from (4)

$$\sigma_{\langle x_0^2 \rangle} = \sqrt{C_{11}}, \quad \sigma_{\langle x_0 x_0' \rangle} = \sqrt{C_{22}}, \quad \sigma_{\langle x_0'^2 \rangle} = \sqrt{C_{33}}. \quad (7)$$

After the initial correlations are found, the Twiss parameters emittance, alpha, and beta are defined by equations

$$\varepsilon = \sqrt{\langle x_0^2 \rangle \langle x_0'^2 \rangle - (\langle x_0 x_0' \rangle)^2}, \quad (8)$$

$$\alpha = -\langle x_0 x_0' \rangle / \varepsilon, \quad (9)$$

$$\beta = \langle x_0^2 \rangle / \varepsilon. \quad (10)$$

The error of any scalar function of initial correlations  $f(\vec{t})$

$$\vec{t} = [\langle x_0^2 \rangle, \langle x_0 x_0' \rangle, \langle x_0'^2 \rangle]^T \quad (11)$$

is given by

$$(\sigma(f))^2 = (\nabla_{\vec{t}} f)^T \cdot C \cdot (\nabla_{\vec{t}} f). \quad (12)$$

Formulas (7) are special cases of this general formula. It also allows estimating the errors for the initial Twiss parameters (8-10).

All together formulas (4 – 12) describe the transverse profiles analysis including the error analysis.

### Space Charge Effects

In the presence of space charge the transport matrices in (2) will be dependent on the initial Twiss parameters for the longitudinal and transverse directions. As for the longitudinal Twiss parameters, there are several possible ways to find the initial values. First, we can blindly use the design parameters. Second, for the SCL we can use the methods described in this paper later. For the transverse parameters the transport matrices dependency makes the equation (2) a transcendental one, and there is no exact analytic solution for it.

To solve (2) in the presence of the strong space charge a two steps method was used. In the beginning, a general nonlinear fitting package was used to find the initial parameters that will minimize the S function (3). Then the transport matrices generated by the OM for these initial Twiss parameters were used in (4) and (7) to get a new set of these parameters and their error estimation. If these two sets were close enough assuming their errors, we concluded that the problem is solved. This method does not guarantee a uniqueness of the solution, because the fitting routine can find several local minima. This situation can be resolved by increasing the number of measurements with the lattice configurations providing the reduced errors (7). These additional measurements should be planned ahead by using the preliminary estimation for the initial Twiss. The rule of thumb from [5] is a  $90^0/(N-1)$  betatron phase advance distance between each measurement. The exact effect of each additional measurement should be estimated by (7). Unfortunately, even these measures cannot guarantee a uniqueness of the solution and correctness of the error estimation.

### Twiss Parameters Correlations

The diagonal elements of the covariance matrix  $C$  (6) include information about errors of  $\langle x_0^2 \rangle$ ,  $\langle x_0 x'_0 \rangle$ , and  $\langle x_0'^2 \rangle$  parameters (7), and the non-diagonal elements of  $C$  describe their correlations. The graphical representation of these correlations on two dimensional plots like the  $(\beta, \epsilon)$  plane could be very beneficial. As we will show later, sometimes it helps to explain the nature of very high errors of the Twiss parameters. The algorithm for plotting these correlations starts with the diagonalization of  $C$

$$C = (M^T W M)^{-1} = V \cdot D \cdot V^T, \quad (13)$$

where  $D$  is a diagonal matrix, and  $V$  is a transformation matrix for the  $\langle x_0^2 \rangle$ ,  $\langle x_0 x'_0 \rangle$ , and  $\langle x_0'^2 \rangle$  parameters to a new set of variables  $\vec{\theta}$

$$\vec{\theta} = V^T \cdot \vec{\tau}, \quad \vec{\tau} = [\langle x_0^2 \rangle, \langle x_0 x'_0 \rangle, \langle x_0'^2 \rangle]^T. \quad (14)$$

For  $\vec{\theta}$  the covariance matrix  $D$  is diagonal. Therefore, the errors of  $\vec{\theta}$  are defined by the diagonal elements of  $D$  (similar to (7)), and they are not correlated. The possible values of  $\vec{\theta}$  are inside the rectangular region with the center defined by (14) and widths  $[2 \cdot \sqrt{D_{11}}, 2 \cdot \sqrt{D_{22}}, 2 \cdot \sqrt{D_{33}}]$ . The surface points of this region can be easily projected onto any planes representing Twiss parameters correlations.

### SCL LASER WIRE PROFILES ANALYSIS

To measure the transverse beam profiles in the SNS superconducting linac we use Laser Wire (LW) stations [6] instead of traditional wire scanners. LW stations perform nonintrusive measurements based on a photo-detachment process. The scans can be done even during 1 MW operation. The dynamic range of the LW measurement is lower than the traditional wire scanners, so in our analysis we used only beam sizes calculated as a Gaussian fit to the profiles. Figure 2 shows a typical laser wire profile with a fit, and the high level of noise does not allow us to calculate RMS of the profile directly. All measurements discussed in this section were performed in 2011 and 2012. Since then the SCL LW system was significantly improved [6].

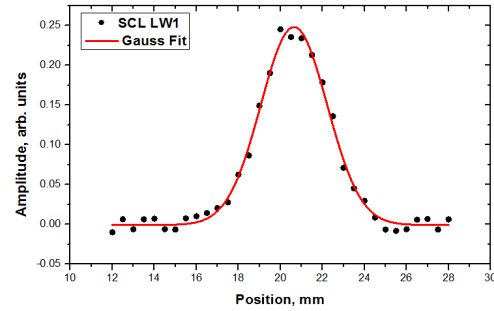


Figure 2: LW1 profile measurement and a Gaussian fit.

Earlier we reported that our attempts to improve SCL beam size beating failed because we could not find the initial Twiss parameters at the entrance [7]. After applying the analysis described in the previous section, it was found that the Twiss parameters errors were too big to make any meaningful conclusions. The detailed study of these errors showed the strong correlation between the emittance and Twiss beta parameter values.

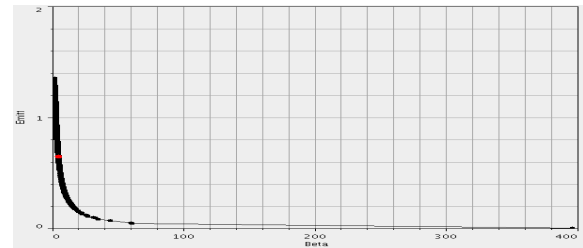


Figure 3: A correlation between the emittance and the beta Twiss parameter. The red dot is a central point found in the nonlinear fit.

As example, Fig. 3 shows this correlation with the region calculated with formulas (13) and (14) from the “Twiss Parameters Correlations” section of this paper. The possible range for the emittance is from almost 0 to  $1.4 \pi \cdot \text{mm} \cdot \text{mrad}$  and the beta parameter is from 0 to 400 m. The beta range could be narrowed down if the emittance value is considered as a known parameter.

The initial transverse Twiss parameters measurement was improved after the error control (formulas (6) and (7) and multiple lattice configurations) was implemented. It

was found that the quad gradients should be increased by 10% -15% to reduce the error to an acceptable level.

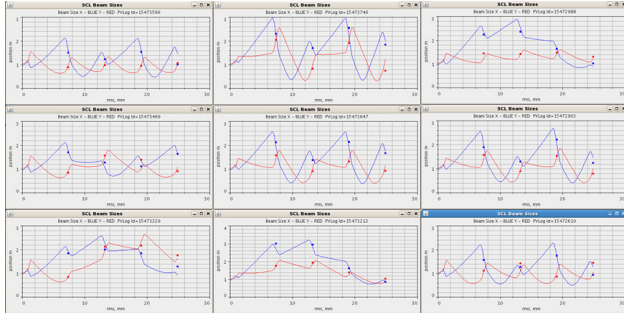


Figure 4: Transverse beam sizes at first 4 LW stations in SCL for 9 different quad settings. Blue and red colors are for horizontal and vertical directions respectively. Points are LW results, and curves are the model with the same initial Twiss.

Figure 4 shows the excellent agreement between LW measurements and the OM simulations for 9 lattice settings. These data were taken for all SCL cavities switched off and a low peak current to eliminate space charge effects. For the production peak currents 28-35 mA and the RF cavities switched on the agreement between the model and LW data was good for the first three LW stations. The measured transverse Twiss parameters at the entrance of SCL for the production tune for 37 mA peak current are shown in Table 1 (emittance normalized, rms). Unfortunately, we could not predict the transverse beam sizes downstream for the whole SCL linac. At that moment, we realized that we need more precise information about the longitudinal Twiss parameters and a verified model for the longitudinal dynamics calculations. The next section will describe our approach to this problem.

Table 1: Transverse Twiss Parameters

Direction	Alpha	Beta [m]	Emittance $\pi^*mm^*mrad$
Horizontal	$-0.55 \pm 0.22$	$2.35 \pm 0.84$	$0.40 \pm 0.08$
Vertical	$0.66 \pm 0.14$	$7.7 \pm 1.8$	$0.38 \pm 0.05$

## LONGITUDINAL TWISS PARAMETERS

Recently at SNS, a new method of measuring of the rms longitudinal Twiss parameters of a beam in linear accelerators was developed [8]. The method is based on using sum signals from BPMs sensitive to the longitudinal charge distribution in the bunch. The applicability of the method was verified with direct longitudinal profile measurements by the Bunch Shape Monitor (BSM) at the end of Coupled Cavity Linac (CCL) which is a part of the linac preceding the SCL. The method is fast and simple, and can be used in linear accelerators where interceptive diagnostics are not desirable. The previously developed method based on

transmission and beam loss measurements [7, 9] is less accurate and is much more time and effort consuming.

The new method is based on the same formulas (2-10), and the BPMs are used to measure the longitudinal rms sizes.

### BPM and Longitudinal RMS Size of Bunch

At the SNS linac the sum signal of a BPM is proportional to the Fourier amplitude of the longitudinal bunch distribution at the frequency of the BPM system

$$u = J \cdot \zeta \cdot 1/I_0 \left( \frac{\omega R}{\gamma \beta c} \right), \quad (15)$$

where  $J$  is an amplitude of the beam current harmonic at the BPM frequency  $\omega$ ;  $\zeta$  is a factor describing the transfer function of the BPM including the pickup geometry, amplifier gain etc.;  $R$  is the radius of the pickup aperture;  $c$  is the speed of light;  $\beta$  and  $\gamma$  are relativistic factors; and  $I_0$  is the modified Bessel function. In the case of Gaussian longitudinal bunch shape

$$u = Q \cdot \zeta \cdot \exp\{-\omega s_z)^2/2\}/I_0 \left( \frac{\omega R}{\gamma \beta c} \right), \quad (16)$$

where  $Q$  is the total charge of the bunch and  $s_z$  is the RMS bunch time length. The calibration constant ( $Q \cdot \zeta$ ) can be measured as BPM amplitude at the production SCL tune when  $\omega s_z \ll 1$ . Inverting equation (16) with respect to  $s_z$  we get the bunch length from the BPM sum signal for formulas (2-10).

The main assumption that was used for the formula (16) is a Gaussian shape of the longitudinal density of the bunch. Figure 5 shows the longitudinal bunch distribution at the end of CCL which has an almost perfect Gaussian shape. For the production tune, during the acceleration of the bunch by SCL cavities, we keep the bunch short enough to avoid non-linear distortion from the cavities and beam loss. Therefore, we are confident that we keep the Gaussian shape of the bunch through the whole SCL.

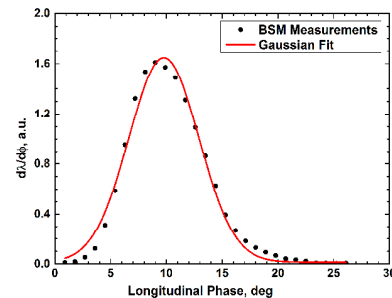


Figure 5: The longitudinal beam profile measured by the BSM in the CCL.

### Longitudinal Twiss Parameters Analysis

In [8] it is shown that a simple measurement with a coasting beam is not accurate enough to get useful initial longitudinal Twiss parameters. The errors of these parameters are too big. As a solution, it was suggested to use a phase scan of the RF cavity placed between the initial point and the BPMs. In the case of the phase scan, the number of different longitudinal transport matrices  $m^{(i)}$  in (2) increased to  $N_\phi \times N_{BPM}$  where  $N_\phi$  and  $N_{BPM}$

are the number of the cavity phase points and the number of BPMs, respectively. For a phase scan step of  $5^{\circ}$   $N_{\phi} \times N_{BPM} = 72 \times 15 = 1080$  measurements. It is also important that during the scan the cavity performs different focusing-defocusing transformations with the bunch in the longitudinal phase space. Fortunately, we already have the results of the phase scans of all SCL cavities that we used to initialize the SCL lattice of the OM model. A picture of the BPM amplitudes during the phase scan of the first SCL cavity is shown in Fig. 6.

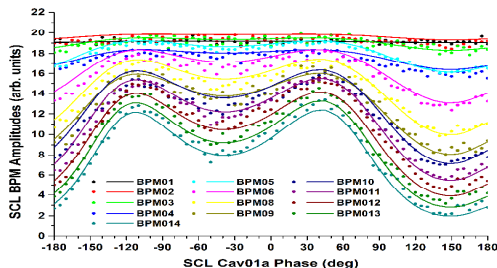


Figure 6: The BPM amplitudes during a Cav01a phase scan. Points are measurements, lines are from OM model.

The phase scan data were taken at the peak current of 30 mA which is different from the 37 mA during the transverse Twiss measurements, but we used the same transverse Twiss parameters anyway. This makes our analysis somewhat inconsistent, and in the future we plan to perform transverse and longitudinal analysis on the same set of data. After the analysis, we found longitudinal Twiss parameters at the entrance of the first SCL cavity are  $\alpha = -0.78 \pm 0.02$ ,  $\beta = 8.1 \pm 0.2$  [m/rad],  $\epsilon = 0.60 \pm 0.01$  [ $\pi \cdot \text{mm} \cdot \text{mrad}$ ] (XAL OM units).

Then we performed the same analysis for each SCL cavity in the Medium Beta section (unfortunately we scanned only this part). This gave us measured longitudinal Twiss parameters along the SCL. We also used the initial Twiss and the initialized OM lattice to simulate the same parameters. The Twiss parameters obtained two ways are shown in Fig. 7.

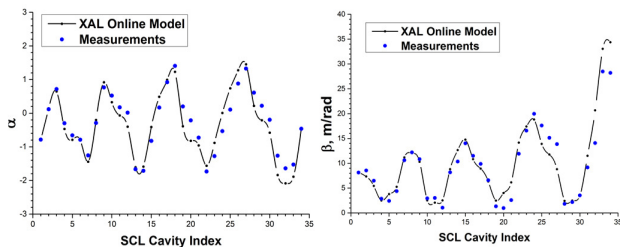


Figure 7: The longitudinal Twiss  $\alpha$  and  $\beta$  parameters along SCL.

We have a relatively good agreement between the measured and simulated Twiss, but they do not agree inside error bars. The differences can be explained by the very strong longitudinal over-focusing of the bunch where the space charge effects are strong and the envelope model could be less accurate. Figure 7 demonstrates a

poor matching in the longitudinal direction for the existing SCL tune.

## CONCLUSIONS

The practical approach to the 3D beam characterization is suggested and tested on the example of the SNS superconducting linac. The new method of the longitudinal Twiss parameters measurement is developed and used. This is the first time the longitudinal parameters have been measured continuously along the linac. The role of the space charge effects should be studied further. The applicability of the XAL OM for the linac tuning is demonstrated.

## ACKNOWLEDGMENT

The author is grateful to the members of SNS Beam Instrumentation team A. Aleksandrov, Y. Liu, and C. Long for the help in data acquisition and useful discussions.

ORNL/SNS is managed by UT-Battelle, LLC, for the U.S. Department of Energy under contract DE-AC05-00OR22725.

## REFERENCES

- [1] V. Lebedev et al., LINAC2010, Tsukuba, Japan, p. 929 (2010).
- [2] A. Shishlo et al., Phys. Rev. Lett. 108, 114801 (2012).
- [3] C. K. Allen, C. A. McChesney, C. P. Chu, J. D. Galambos, W.-D. Klotz, T. A. Pelaia, and A. Shislo, "A Novel Online Simulator for Applications Requiring a Model Reference," ICALEPCS 2003 Conference Proceedings, Kyongju, Korea, October 13-17, p. 315 (2003).
- [4] K. R. Crandall and D. P. Rusthoi, Los Alamos National Laboratory Report No. LA-UR-97-886, 1997, <http://laacgl.lanl.gov/laacg/services/traceman.pdf>
- [5] M. G. Minty, F. Zimmermann, "Measurements and Control of Charged Particle Beams," Springer-Verlag Berlin Heidelberg 2003, "Particle Acceleration and Detection" series. p. 104.
- [6] Y. Liu et al., Phys. Rev. ST Accel. and Beams 16 (2013) 012801.
- [7] Y. Zhang, "Experience and lessons with the SNS superconducting linac," Proceedings of IPAC'10, Kyoto, Japan, p. 26 (2010).
- [8] A. Shishlo, A. Aleksandrov, Phys. ST Accel. and Beams 16 (2013) 062801.
- [9] Y. Zhang et al., Phys. Rev. ST Accel. Beams 11 (2008) 104001.